Electronic Supplementary Material (ESI) for New Journal of Chemistry.

Supporting Information

A highly selective and sensitive chemosensor for L−tryptophan by employing Schiff based Cu(II) complex

Anoop Kumar Saini,[a] Mohit Saraf,[b] Pratibha Kumari,[c] and Shaikh M. Mobin*[a,b,c]

[a]Discipline of Chemistry, [b]Discipline of Metallurgy Engineering and Materials Science, [c]Discipline of Biosciences and Bio-Medical Engineering, Indian Institute of Technology Indore, Simrol, Khandwa Road, Indore 453552, India

*Email: xray@iiti.ac.in

Tel: +91 731 2438 752

Table S1. Selected bond lengths (Å) and bond angles (º) of **1**.

Bond Distances	**1**
Cu(1)-O(1)	1.895(5)
Cu(1)-O(2)	1.909(5)
Cu(1)-N(1)	1.958(6)
Cu(1)-N(3)	1.962(6)
Cu(2)-O(3)#1	1.901(4)
Cu(2)-O(3)	1.901(4)
Cu(2)-N(5)	1.958(5)
Cu(2)-N(5)#1	1.958(5)

Bond angles	**1**
O(1)-Cu(1)-O(2)	167.4(3)
O(1)-Cu(1)-N(1)	91.7(2)
O(2)-Cu(1)-N(1)	90.7(2)
O(1)-Cu(1)-N(3)	90.7(2)
N(1)-Cu(1)-N(3)	166.7(3)
O(3)#1-Cu(2)-O(3)	162.4(3)
O(3)#1-Cu(2)-N(5)	91.1(2)
O(3)-Cu(2)-N(5)	90.91(19)
O(3)#1-Cu(2)-N(5)#1	90.91(19)
O(3)-Cu(2)-N(5)#1	91.1(2)
N(5)-Cu(2)-N(5)#1	166.5(3)

Table S2. Hydrogen bonding of **1** [Å and (º)].

	D-H...A	d(D-H)	d(H...A)	d(D...A)	<(DHA)
1					
1	C(5)-H(5)…O(3)#(1)	0.950(.000)	2.665(.000)	3.384(.000)	132.85(0.00)

Equivalent positions:

(1) x,+y-1,+z

Table S3. Electronic properties of **1**.

Compound	$\lambda_{(S0\rightarrow S1)}$ (nm)	ε (M^{-1} cm^{-1})
1	307	4.6×10^3
	388	2.1×10^3
	405	2.0×10^3

Table S4 Comparison table of some previously reported L−Trp sensors.

Electrode Material	**LOD (nM)**	**Sensitivity ($\mu A\ \mu M^{-1}cm^{-2}$)**	**Oxidation Potential (V)**	**References**
Multiwall carbon nanotube/Mg-Al layered double hydroxide	6.8	-	0.639	*J. Electroanal. Chem.*, 2013, **704**, 220-226.
Flower-like structured nanocomposite consisting of reduced graphene oxide and SnO_2	40	37.3	0.76	*Sens. Actuator B- Chem.*, 2017, **239** 1221-1230.
Silver nanoparticle-graphene nanocomposite	2	-	0.8	*Biosens. Bioelectron.,* 2013, **42**, 198-206.
Electrospun tricobalt tetroxide nanoparticles decorated carbon nanofibers	200	-	0.85	*Sens. Actuator B-Chem.,* 2017, **241**, 601-606.
Gold nanoparticles/poly(alizarin red S)	6.7	-	~0.7	*J. Solid State Electrochem.*, 2013, **17**, 2623-2631.
Reduced graphene oxide polymer nanocomposite	316	0.0451	0.728	*Sens. Actuator B-Chem*., 2016, **233**, 445-453.
Silver nanoparticles/metal-organic framework composite	140	-	0.989	*RSC Adv*., 2016, **6**, 13742-13748.
β-Cyclodextrin/Fe_3O_4 hybrid magnetic nano-composite	500	-	0.8	*Sens. Actuator B-Chem.*, 2012, **163**, 171-178.
Graphene oxide hybrid	8	-	0.7	*Analyst* 2015, **140**, 5295-5300.
1	**185**	**3.156**	**0.32**	**Present Work**

Table S5. Real sample analysis performed for ***1-GCE*** (n =3)

Real Sample	**Added (µM)**	**Found (µM)**	**Recovery (%)**
Milk	2.0	1.92	96
	4.0	3.98	99.5
	6.0	6.12	102
	8.0	8.34	104
	10	10.6	106

Table S6. Molecular docking of **1** with xylanases from *B. Circulans*, RNA polymerase PA subunit of avian influenza H5N1 virus, ascorbate oxidase and soybean beta-amylase.

Compound	Protein (PDB Id)	Binding energy (Kcal/Mol)	Inhibition constant	Interacting residues
1	Xylanases from *B. Circulans* **(1XNB)**	-9.07	224.13nM	Chain A: Try5, Gln7, Asn8, **Trp9**, Tyr69, **Trp71**, Pro116, Ser117, Gly120, Asp121, Tyr166
1	Polymerase PA_C-PB_N complex from an avian influenza H5N1 virus (**3CM8**)	-9.12	207.63nM	Chain A: Arg279, Asn466, Lys574, **Trp577**, Ser648, Leu649, Ala651, Ser652, Pro653
1	Ascorbate oxidase from Zucchini **(1AOZ)**	-8.17	1.03 µM	Chain A: Ile161, Arg162, **Trp163**, Arg285, Gln 353, Val355,Val360, **Trp362**, Met 437, Glu443, His512
1	Soybean beta-amylase **(1BYB)**	-7.52	3.06 µM	Chain A: Val99, Gly100, Tyr192, Gln194, **Trp198**, Phe200, **Trp301**, Gln351, Leu383

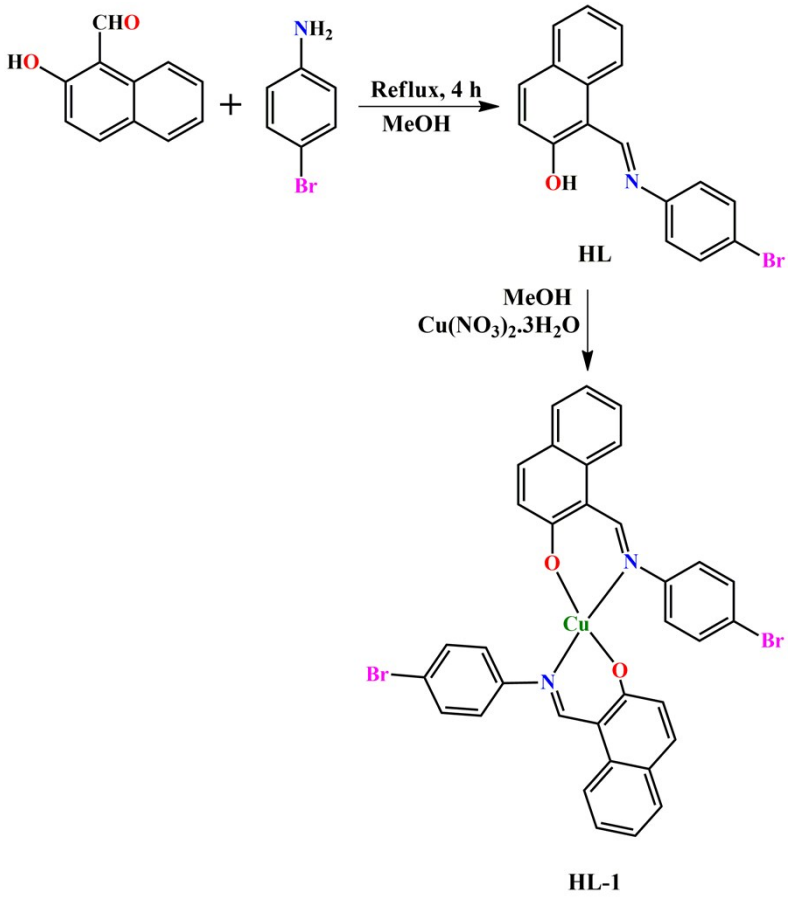

Scheme S1. Synthesis of ligand HL and HL-1.

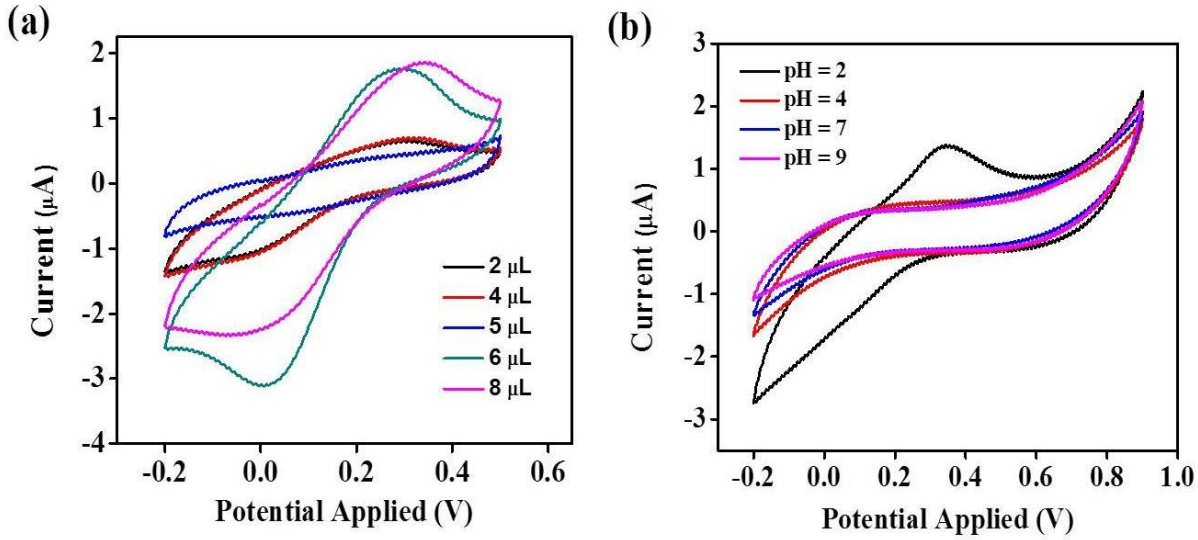

Fig. S1. CV profiles of ***1*−*GCE*** at (**a**) different mass loadings and (**b**) different pH.

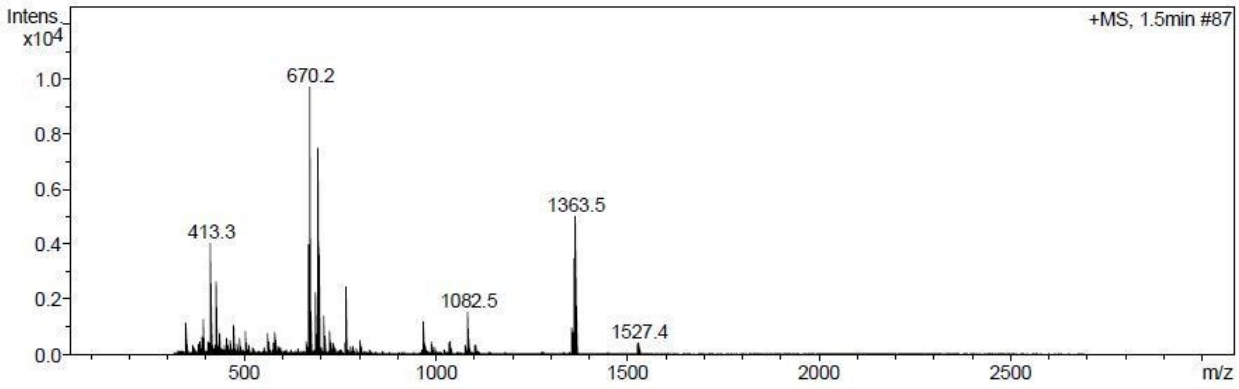

Fig. S2. ESI–MS spectrum of **1**.

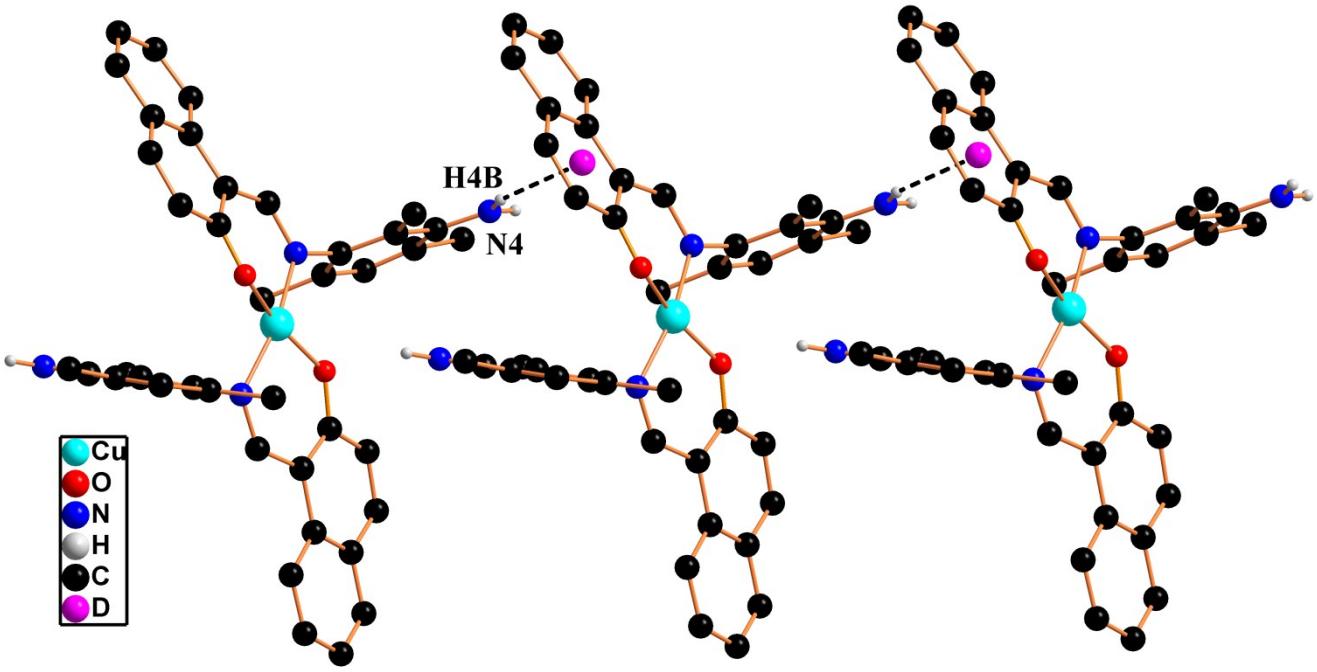

Fig. S3. N−H···π interactions in **1** forming 1D−polymeric chain (black dotted line), where D represent the dummy atom.

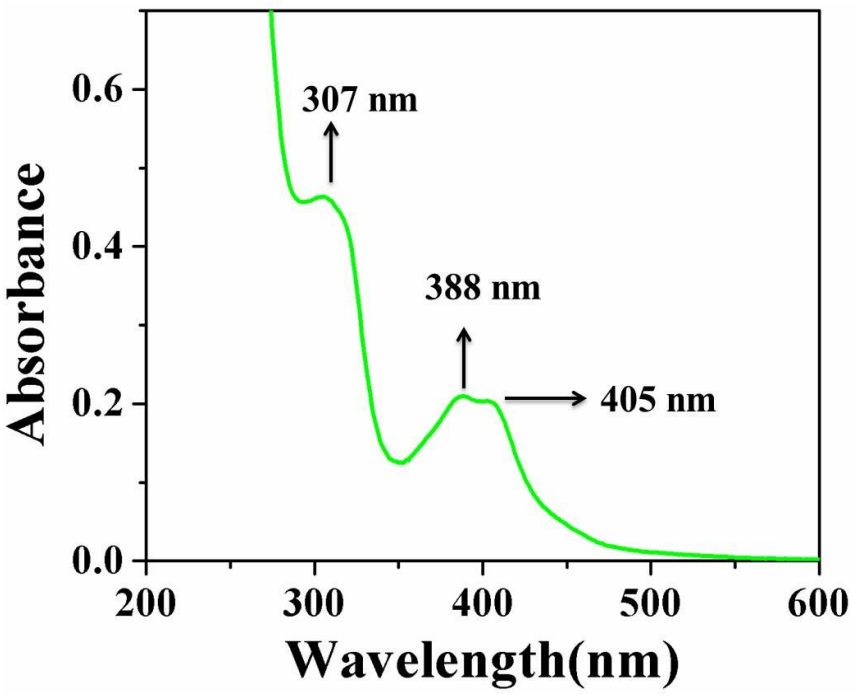

Fig. S4. Absorption spectrum of **1** in $CHCl_3$ ($c = 1.0 \times 10^{-5}$ M).

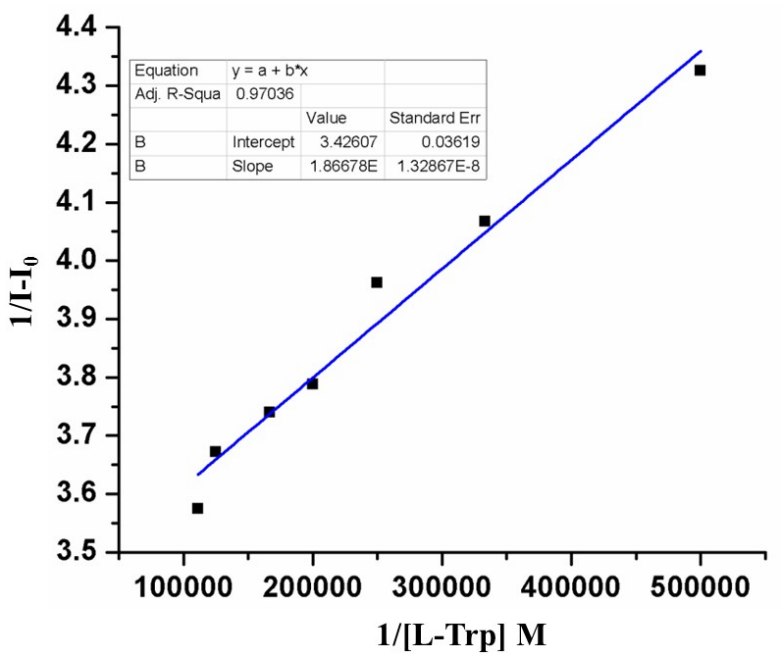

Fig. S5. Bensei-Hildbrand plot (B-H plot) obtained from absorption (at 430 nm wavelength) studies. The binding affinity is $K_a = 1.88 \times 10^5\ M^{-1}$

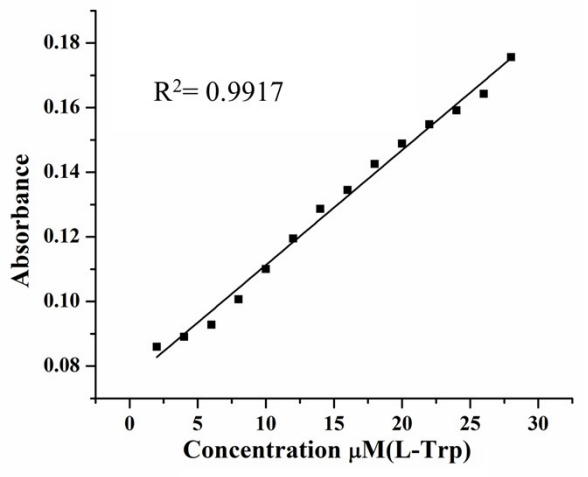

Fig. S6. Calibration curve for the determination of L-Trp, at λ_{max}= 430 nm (LOD = 124 nM).

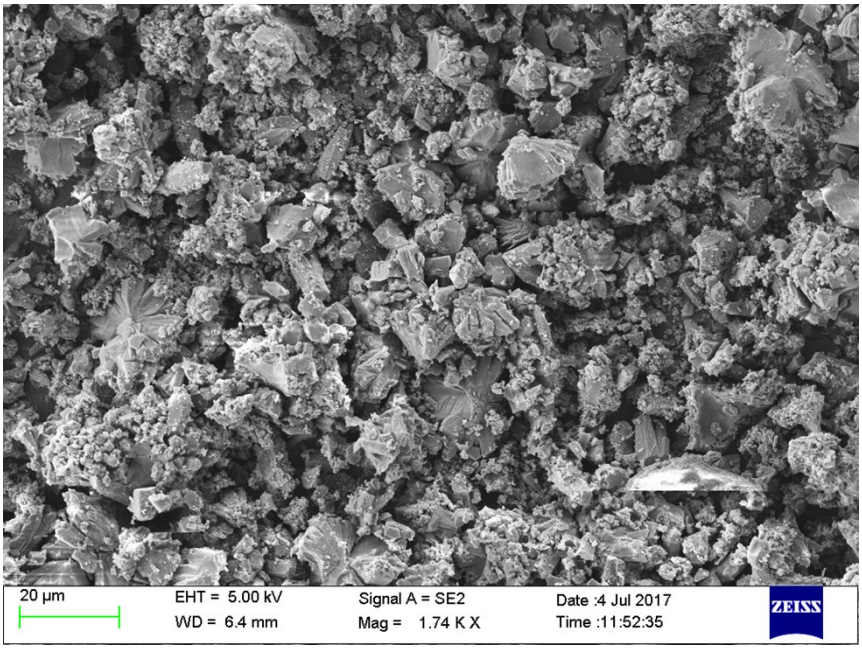

Fig. S7. SEM image of ***1-GCE***.

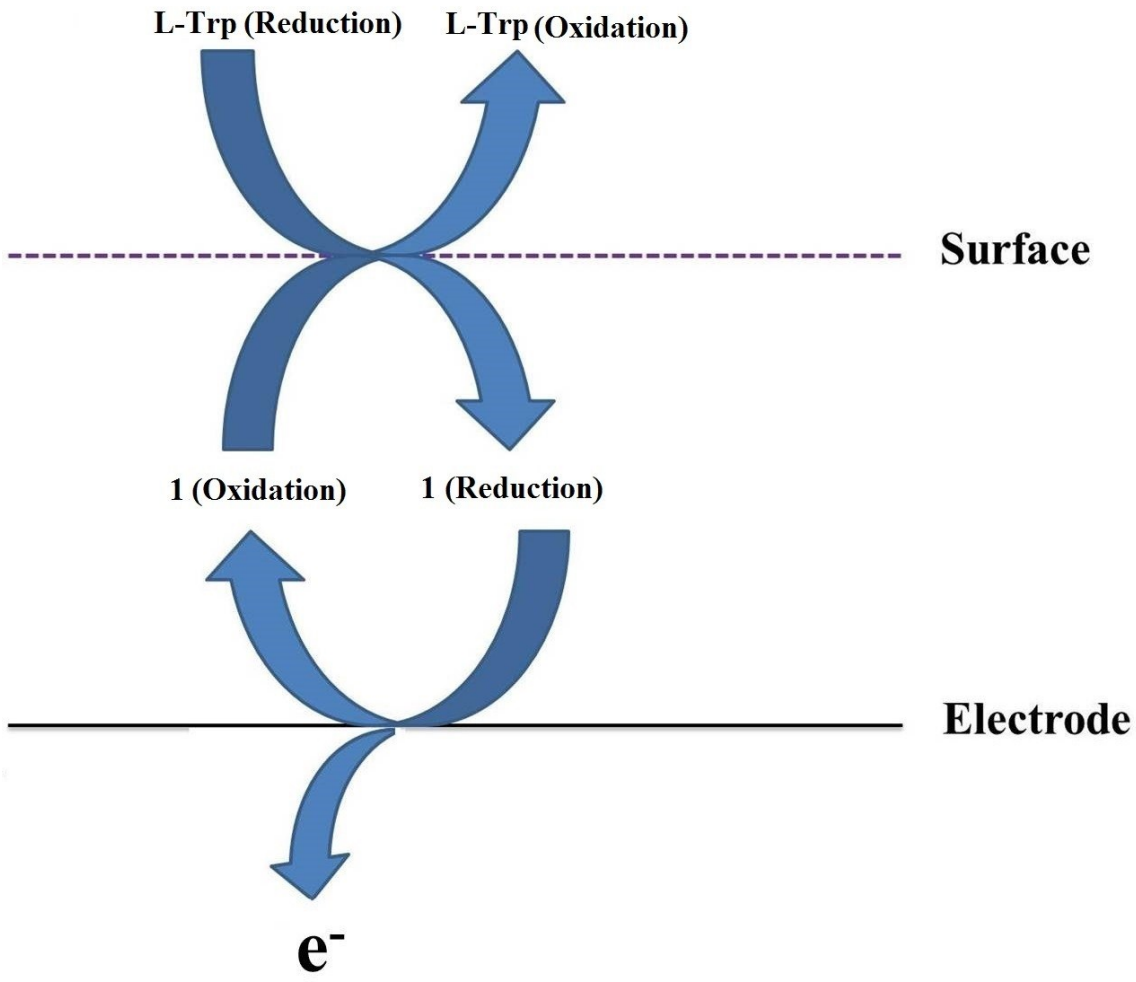

Fig. S8. Operational mechanism of the proposed sensor.

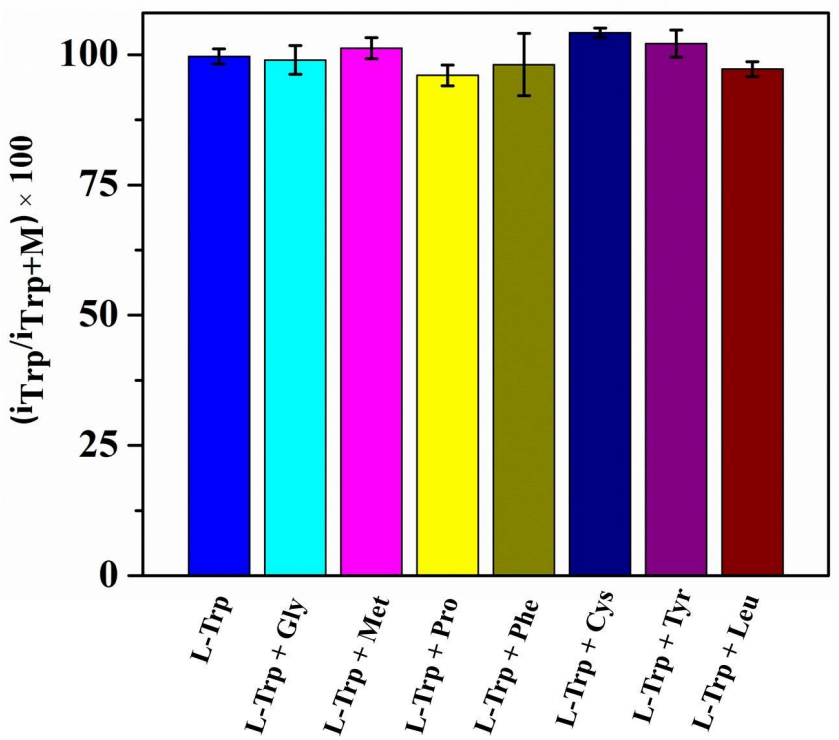

Fig. S9. Selectivity study of ***1-GCE*** in the determination of L-Trp.

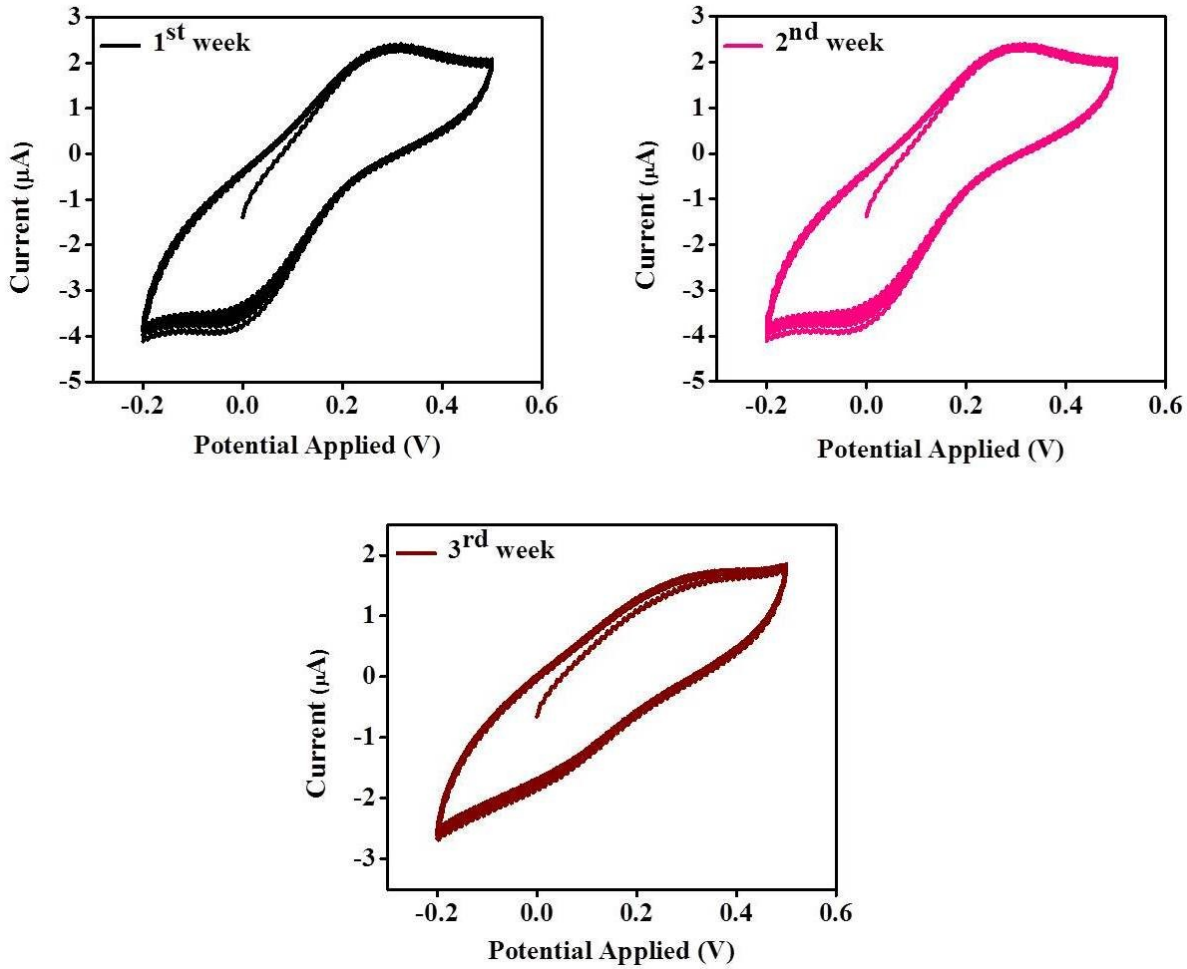

Fig. S10. CV responses (20 cycles) for ***1−GCE*** recorded up to three weeks.

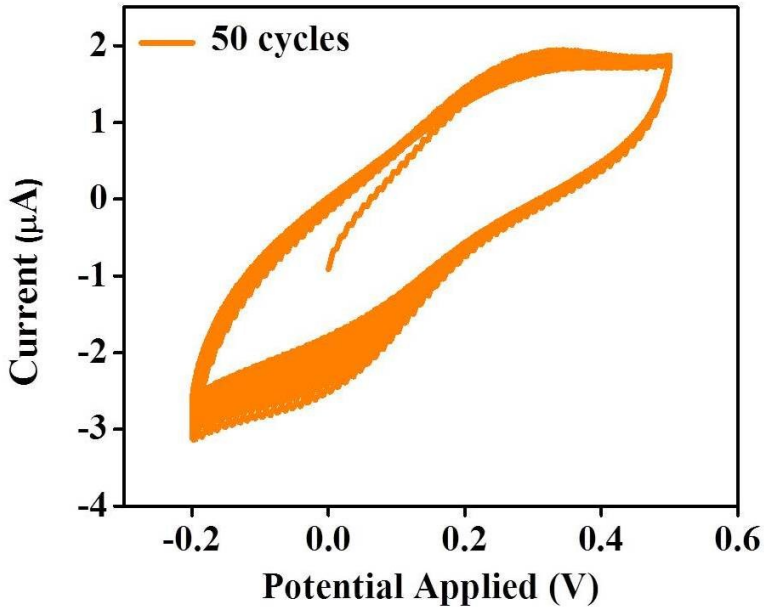

Fig. S11. CV response (50 cycles) for ***1−GCE*** recorded after three weeks.

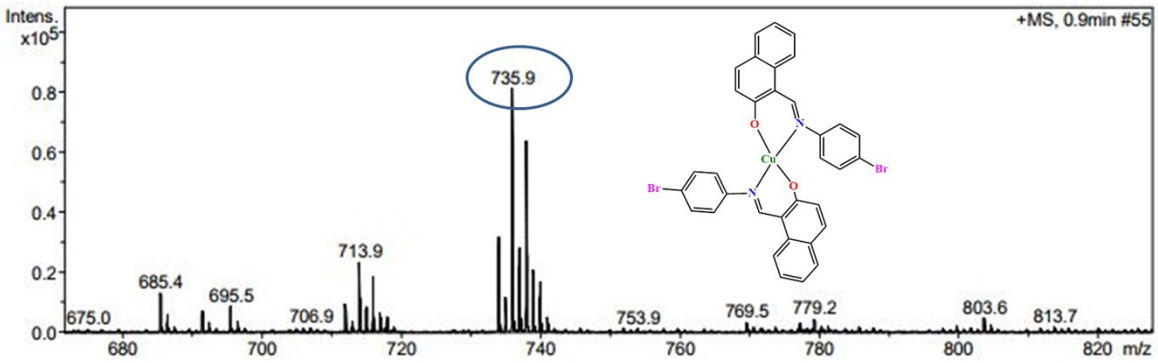

Fig. S12. ESI–MS spectrum of **HL-1** (M+Na).

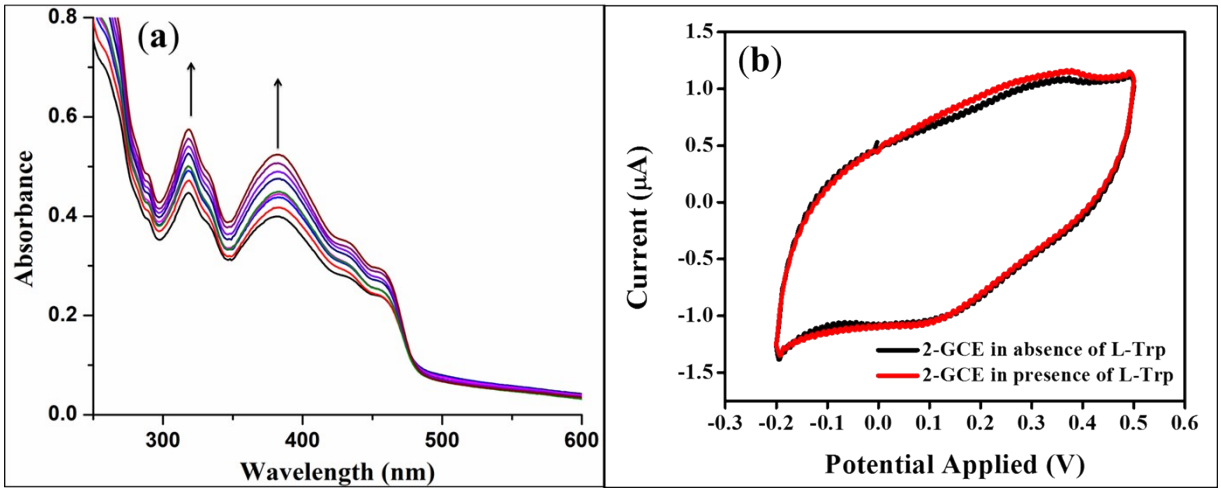

Fig. S13. (**a**) UV/vis absorption titration spectra of HL−1 (c = 1.0 × 10^{-5} M) in aq. ACN (ACN/H_2O = 7:3 v/v, 10 μM phosphate buffer, pH = 7.0) with L−Trp (c = 1.0 × 10^{-4} M). (**b**) CV profiles of ***2-GCE*** in the presence and absence of L-Trp.

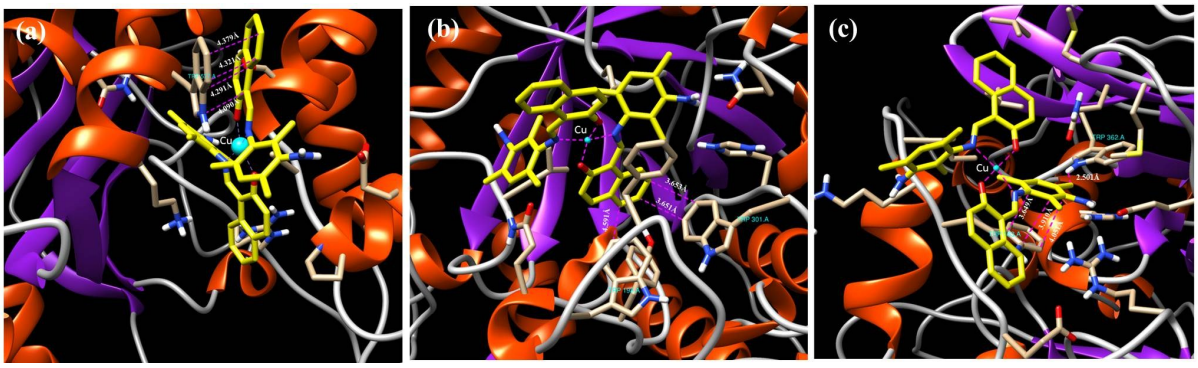

Fig. S14. Molecular docking of **1** with various proteins. Protein represented as ribbon (β – sheet: purple, helix: red and coil: grey) interacting residues within 5Å represented as stick. **1** is shown as stick (yellow colour). π–π stacking interaction are shown as dotted line (purple) between Trp and **1**. (**a**) RNA polymerase subunit of influenza virus H5N1 (PDB: 3CM8), **Trp755** residue form π–π stacking integration with naphthyl ring of **1** (4.379Å, 4.321Å, 4.291Å, 4.090Å). (**b**) soybean beta-amylase (PDB:1BYB), **Trp301** residue show π–π stacking integration with **1** (3.653Å, 43.651Å). (**c**) ascorbate oxidase (PDB:1AOZ), Indole ring of **Trp163** form π–π stacking interaction with mesitylene ring of **1** having bond distance 3.649Å, 3.910Å, 4.051Å.